

Carbon Stock Estimation From Vegetation Biomass Using Spot-7 Imagery

Iklila Rahmatika¹, Iswari Nur Hidayati¹, R. Suharyadi¹, Emilya Nurjani¹

¹Faculty of Geography, Gadjah Mada University, Indonesia

Submit : 2022-10-27

Received: 2023-02-16

Accepted: 2023-04-06

Keywords: biomass;
remote sensing; SPOT-7;
carbon stock; Yogyakarta

Correspondent email :

iklilarahmatika99@gmail.com

Abstract Vegetation absorbs carbon dioxide (CO₂) emissions during photosynthesis. Covering more areas with trees will increase the CO₂ absorption capacity more substantially than other vegetation like bushes, grasses, or rice fields. Trees convert the CO₂ captured during photosynthesis into organic carbon to be stored in biomass. Woody trees account for approximately 60% of the total aboveground tree biomass, and trunks, where food reserves produced in photosynthesis are stored, have relatively large biomass compared to other parts of the tree. The biomass of a vegetation stand determines the optimization of air pollutant absorption in urban areas. Yogyakarta City is the center for tourism, education, and cultural activities in Indonesia, which is vulnerable to land-use conversion, a factor of the shrinking green space. This study aimed to estimate carbon stock from vegetation biomass in Yogyakarta City using the remote sensing product SPOT-7 imagery. To calculate the vegetation biomass, the diameter at breast height (DBH) of stands was measured in the field. Then, statistical analyses were performed to determine the correlation and regression between the actual or observed biomass and the Normalized Difference Vegetation Index (NDVI) value derived from the SPOT-7 image. The regression model used was $y = 1.4277x - 0.0849$. The total biomass produced in Yogyakarta City was estimated at 1,399,487.1 tonnes, which contained 643,764.1 tonnes of carbon stock.

©2023 by the authors. Licensee Indonesian Journal of Geography, Indonesia.

This article is an open access article distributed under the terms and conditions of the Creative Commons Attribution (CC BY NC) license <https://creativecommons.org/licenses/by-nc/4.0/>.

1. Introduction

Vegetation is a group of plants that jointly occupy an area and interact with each other and their environment as part of land cover. Vegetation absorbs CO₂ emissions during photosynthesis. As such, it positively affects air quality both directly and indirectly by changing the atmospheric conditions of its surroundings (Irawan and Sirait, 2018). For instance, denser vegetation makes an area more liveable (Yanti et al., 2020), and maintaining its existence can prevent environmental damage and even disasters. Based on research by Mansur and Pratama (2014), different species of plants have different heights, diameters, leaf thicknesses, and CO₂ absorption capacities. Covering more areas with trees will increase the absorption capacity more substantially than other vegetation like bushes, grasses, or rice fields (Handayani et al., 2020). Woody trees account for approximately 60% of the total aboveground tree biomass, and the trunk, where food reserves produced in photosynthesis are stored, has a fairly large biomass compared to other parts of the tree (Brown, 1997). Based on these statements, it can be concluded that species dictate variations in the physical characteristics of leaves, stems, and other parts of vegetation. This affects plant density and its ability to capture pollutants in the air.

Biomass is defined as a form of carbon stock that can be quantified from at least four carbon pools: aboveground biomass, belowground biomass, dead organic matter, and soil organic carbon, which is expressed in tonnes of dry weight per unit area (Brown, 1997; Sutaryo, 2009). This research calculates aboveground biomass, that is, the trunk of a tree. Trees absorb CO₂ during photosynthesis and convert it into organic carbon (carbohydrates) to be stored in biomass (Sutaryo, 2009).

Therefore, biomass has a vital role in reducing air pollution that is common in urban areas, especially the number of CO₂ pollutants. According to the World Health Organization (WHO), air pollution kills about 7 million people worldwide every year. Exposure to excessive amounts of CO₂ emissions can lead to death (Mukono, 2011). In addition, CO₂ gas is the most significant contributor to global warming, i.e., around 70% (Ayvaz et al., 2017), compared to other greenhouse gases (Lee et al., 2013). Therefore, when more CO₂ is absorbed by vegetation and stored as carbon biomass, this helps control the adverse consequences of the greenhouse effect (Samsudin et al., 2009).

Biomass can be estimated using two methods: direct harvesting (destructive sampling) and indirect harvesting (non-destructive sampling). In destructive sampling, all parts of the plant are harvested, dried, and weighed as biomass (Sutaryo, 2009). Meanwhile, the non-destructive sampling uses allometric equations that are based on the relationship between the diameter at breast height (DBH) and other tree variables. The latter method involves less complicated measurement of the total biomass contained, has higher accuracy, and is more practical for use in potential carbon stock inventory (Brown, 1997). Diameter at breast height (DBH) is the diameter of a trunk measured at breast height or approximately 1.3 m from the ground (Sutaryo, 2009), while allometric equations estimate the biomass of a stand using parameters, such as diameter, height, or their combination (Krisnawati et al., 2012). Therefore, this study used an allometric equation to calculate the tree biomass and field surveys with non-destructive sampling to collect DBH information.

Remote sensing is widely applied to identify phenomena

on the earth's surface. This technology is considered more effective than direct measurements in the field (Sutanto, 1986). Remote sensing data can be the main data source in estimating the carbon stock or biomass of a given area (Lu, 2005) by, among others, combining temporal resolution with statistical methods (Wahyuni, 2012). For instance, the Normalized Difference Vegetation Index (NDVI) values and digital values from remote sensing image bands can be used to generate biomass estimation models (Achmad *et al.*, 2018). In the current study, the biomass estimation relied on the SPOT-7 PMS (panchromatic and multispectral) imagery, whose level of accuracy allows for detailed identification of green open space, a component in the calculation of CO₂ emission absorption, through visual interpretation.

Yogyakarta is the most densely populated city in the Province of D.I. Yogyakarta, Indonesia (BPS, 2021a) and the center of tourism, education, and cultural activities. Yogyakarta City is a popular tourist destination in Indonesia besides Bali (Qanitat, 2016). Palaces, shopping centers, and various museums are among the reasons why more tourists visit the city than other cities/regencies. In 2020, Yogyakarta had a population of 373,589 people occupying an area of 3,250 ha, creating a density of 11,495 people/km² (BPS, 2021b). This figure was the highest among the cities/regencies in the province. According to Lee (2008), rapid population growth in cities causes various problems, such as environmental pollution, reduced open space, poor land development planning, and traffic congestion.

2. Methods

Image Correction

This study used SPOT-7 PMS imagery. SPOT-7 was launched on June 30, 2014, as part of a satellite constellation with SPOT-6. Pansharpened image data were obtained from the National Institute of Aeronautics and Space with a spatial resolution of up to 1.5 m for the panchromatic image and 6 m for the multispectral image. SPOT-7 is suitable for acquiring better knowledge for environmental resource management, identifying and predicting climatic and oceanographic phenomena, and monitoring natural resources and anthropogenic activities (ESA, n.d.).

Prior to use, the SPOT-7 images were radiometrically and atmospherically corrected. The radiometric correction was conducted to improve the display quality of an image and correct image pixel values to match the spectral reflectance value of an actual object in the field (Danoedoro, 2012). This process converts the digital number (DN) in each pixel to top-of-atmosphere (TOA) spectral radiance using GAIN and

BIAS coefficients, producing an image with the unit of watts per steradian per square meter ($W \cdot sr^{-1} \cdot m^{-2}$). The radiance values can be further converted to reflectance; TOA spectral reflectance is the ratio of the normalized TOA spectral radiance to solar irradiance (SPOT 6/7 daya user's community, 2013). The conversion process of DN into TOA spectral radiance can be conducted quickly and automatically in ENVI software, which provides preprocessing tools for radiometric corrections.

The radiometrically corrected image was further processed for atmospheric correction. The radiative transfer model is one of the most commonly used atmospheric correction methods for remote sensing images because it has a high accuracy in reflectivity calculation compared to other methods (Jiaojun *et al.*, 2008). One of the algorithms used in the model is the Moderate Spectral Resolution Atmospheric Transmittance Algorithm and Computer Model (MODTRAN). In ENVI, MODTRAN is provided by Fast Line-of-sight Atmospheric Analysis of Spectral Hypercubes (FLAASH). FLAASH is a program that can perform image corrections by removing the effects of water vapor, atmospheric gases such as oxygen, carbon dioxide, methane, ozone, and molecular and aerosol scattering (Danoedoro, 2012), which then produces a reflectance value that is close to that of the actual object on the earth's surface. FLAASH can substantially reduce the effect of atmospheric disturbance with more accurate parameters of reflectivity, emissivity, surface temperature, and surface physics (Fibriawati, 2016).

In addition, FLAASH has a wide range of applications and is often used to process different types of remote sensing images. For example, using the MODTRAN4 model on FLAASH to perform atmospheric correction on SPOT-5 images, Yunkai and Zeng (2012) obtained effective correction results, i.e., image information with better accuracy than the Quick Atmospheric Correction (QUAC) model. Therefore, this study used FLAASH to atmospherically correct the high-resolution SPOT-7 PMS imagery to obtain better-quality surface reflectance (SR) images where the spectral response of the portrayed object is close to that of the actual one on the earth's surface.

For atmospheric correction, FLAASH requires input data in the form of a TOA spectral radiance image. Consequently, the image with pixel values (DN) was rescaled to TOA spectral radiance—not further converted into reflectance values—and then corrected atmospherically. The parameters used in FLAASH vary across geographies and can include the MODTRAN4 model, sensor's flight altitude, solar elevation angle, surface altitude, visibility, and aerosol type, which

Table 1. Atmospheric correction parameters inputted to FLAASH

Sensor type	SPOT-7 PMS
Satellite's flight altitude	694 km
Surface level	0.113 km
Pixel size	1.5 m
Recording date	March 03, 2021
Recording time	2:28:13 AM
Atmospheric model	Tropical
Aerosol model	Urban
Visibility	12.09 km
Water column multiplier	1.00 km
Aerosol retrieval	none

affect the success of atmospheric correction (Cooley et al., 2002). It requires particular calculations to obtain visibility; this parameter was derived from MODIS with a Dark Target-Deep Blue merged AOD (aerosol optical depth) product at 550 nm, monthly temporal resolution, and 1° spatial resolution. Ideally, the correct AOD value is determined following the day of image acquisition (daily temporal resolution); however, because the date of recording used in this study does not have an AOD value, the monthly average was selected. Visibility in MODTRAN is related to the AOD value at a wavelength of 550 nm. The parameters used in the atmospheric correction of the SPOT-7 image in this study are presented in Table 1.

Vegetation Density

Vegetation density is related to a plant's physical characteristics, which vary across species. Accordingly, different species of plants have different density values. Plant species and density regulate environmental conditions in urban areas primarily because these features determine the absorption rate of pollutants in the air. Vegetation density is the percentage of plant species that grow in a particular area, which can be quantified with the Normalized Difference Vegetation Index (NDVI) (Wahrudin et al., 2019). NDVI can be used as an indicator of biomass and relative greenness and to determine the status (health or density) of vegetation in an area, but it is not directly related to local groundwater availability (Hung, 2000). NDVI is the most popular index in identifying the greenness or abundance of vegetation. According to Leprieur et al. (2000), it has been one of the most widely used vegetation indices to monitor global vegetation cover over the past two decades. Further, NDVI is known to effectively monitor plants and biomass growth from year to year (Huete et al., 2002; Wang et al., 2005 in Jensen, 2014). Therefore, this study used NDVI to determine vegetation density.

Vegetation density was observed in the field (actual density) to determine its relationship with the same parameter obtained from using the image processing NDVI (estimated density). During field observations, photos of the canopy on a predefined sample plot were taken using a fisheye lens. The photos were then processed in the Gap Light Analyzer (GLA) software to calculate the percent tree canopy cover. GLA is a computer program that extracts canopy structure and gap light transmission displayed on photos captured with a fisheye lens (Frazer et al., 1999).

Actual Biomass Calculation

The calculation of actual biomass begins with measuring the DBH of tree stands in the field. First, a 3 m x 3 m sample plot was made using raffia strings. Then, the circumference of each stand was measured with a measuring tape 1.3 m above the forest floor. Only woody trees with a diameter of more than 5 cm were measured in the field. This corresponds to Nowak et al. (2013), in which trees with a diameter below 5 cm are not included in the biomass calculation. Finally, the circumference was converted into diameter.

Statistical Analysis

The data derived were tested for normality as part of inferential statistics prior to the correlation and regression analysis. This test produces a significance value that concludes whether or not the data used are normally distributed (Siregar, 2015). Correlation analysis determines the direction and

strength of the correlation between two variables (Wijayanti, 2015), which in this study was conducted for two variable pairs: between the vegetation index NDVI and field-derived canopy density and between NDVI and actual biomass. Regression analysis measures the magnitude of the influence between the variables used. It produces a coefficient of determination or R-squared (R^2) to identify to what extent the independent variable can explain the dependent variable. In this study, a linear regression analysis was conducted to model the effect of an independent variable expressed on the x -axis, i.e., the NDVI value, on a dependent variable on the y -axis, i.e., actual biomass (Solima, 2010). This process generated an NDVI-biomass regression equation, which was later used to estimate biomass from any given NDVI value.

In addition, a model accuracy test was performed to determine the magnitude of the error between the estimated (prediction model) and actual biomass (observed from samples in the field). The test samples were the validation samples that were not used in the modeling. The level of accuracy was determined from the Root Mean Squared Error (RMSE) value, which describes the degree of error in the predictions made. Smaller RMSE values indicate more accurate modeling or prediction results (Zhao et al., 2020), meaning that the closer the resulting RMSE is to 0, the higher the model's accuracy is. The equation used to produce the RMSE value is as follows:

$$RMSE = \sqrt{\frac{\sum(Y - Y')^2}{n}} \dots \dots \dots (2.1)$$

where:

Y' : Predicted value (regression modeling results)

Y : Actual value (field observation)

n : Number of data points

Source: Noor (2018)

Afterward, the RMSE-observations standard deviation ratio (RSR) was calculated to obtain more definitive results. The equation used to calculate the RSR value is as follows:

$$RSR = \frac{\sqrt{\sum(Y - Y')^2}}{\sqrt{\sum(Y - X)^2}} \dots \dots \dots (2.2)$$

where:

Y' : Predicted value (regression modeling results)

Y : Actual value (field observation)

X : Average of the actual value

Source: Moriasi et al. (2007)

Following previous research by Moriasi et al. (2007), the RSR was divided into four categories, as presented in Table 2. More precisely, the method in this study is depicted in a flow diagram in Figure 1.

Table 2. RSR classification of the regression model

RSR value	Category
< 0.50	Very good
0.50–0.60	Good
0.60–0.70	Satisfactory
>0.70	Unsatisfactory

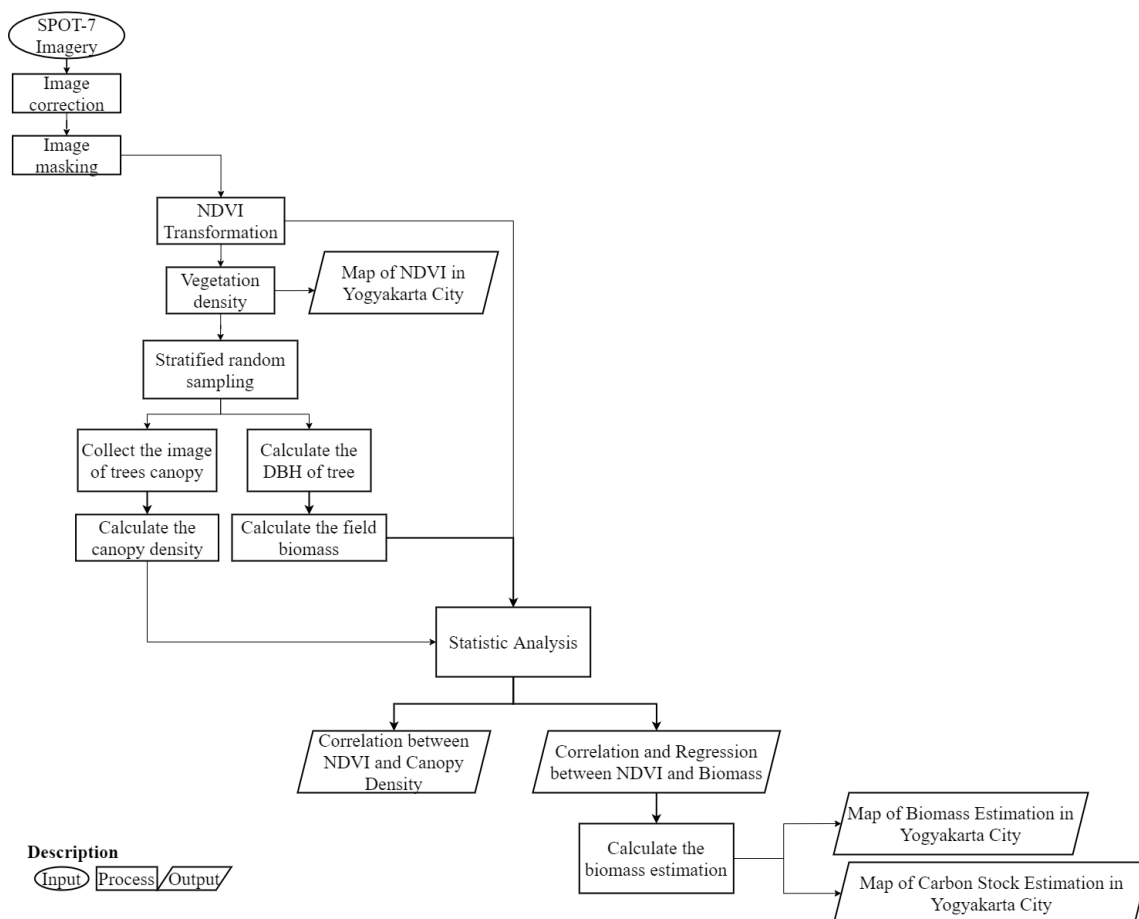


Figure 1. Flow diagram of the research methods

Estimation of Carbon Dioxide Absorption

Table 3. Biomass equation based on climate zones

Rainfall (mm/year)	Climate	Equation	DBH range (cm)
<1.500	Dry	$Y = 10[-0,535 + \log_{10}(BA)]$	3 – 30
1.500-4.000	Humid	$Y = 42,69 - 12,8(DBH) + 1,242(DBH^2)$	5 – 148
>4.000	Wet	$Y = 21,297 - 6,93(DBH) + 0,74(DBH^2)$	4 – 112

Biomass was calculated with an allometric equation, which, according to Brown (1997), uses the height instead of the diameter of a tree stand (Margaretha et al., 2013). Brown (1997) further explained that the biomass of woody trees was approximately 60% of the total aboveground tree biomass, and the trunk has a larger biomass than other parts of a tree because it stores food reserves yielded in photosynthesis. The allometric equation varies across climatic zones (Brown 1997). Yogyakarta City has an average rainfall of 2,012 mm/year, indicating humid climate (Table 3). Brown's (1997) allometric equation used in this research is as follows:

$$Y = 42.69 - 12.8(DBH) + 1.242(DBH^2) \dots \dots \dots (2.3)$$

where:

Y : Biomass (kg)
 DBH : Diameter at breast height (cm)

The biomass regression was obtained by analyzing the magnitude of influence between NDVI values and actual

biomass. The resulting regression equation was then used to predict biomass in the entire research area. The SPOT-7 images were processed in ENVI software to produce new images with biomass values. Through biomass, the stored carbon can be identified. As proposed by Mardiana et al. (2018) and Ma et al. (2018), the carbon concentration is 46% of vegetation biomass; in other words, the conversion factor from biomass to carbon content is 0.46. Therefore, this study used either 46% or 0.46 to determine the carbon stored in biomass. The general equation used to calculate the carbon stock was determined using the formula below:

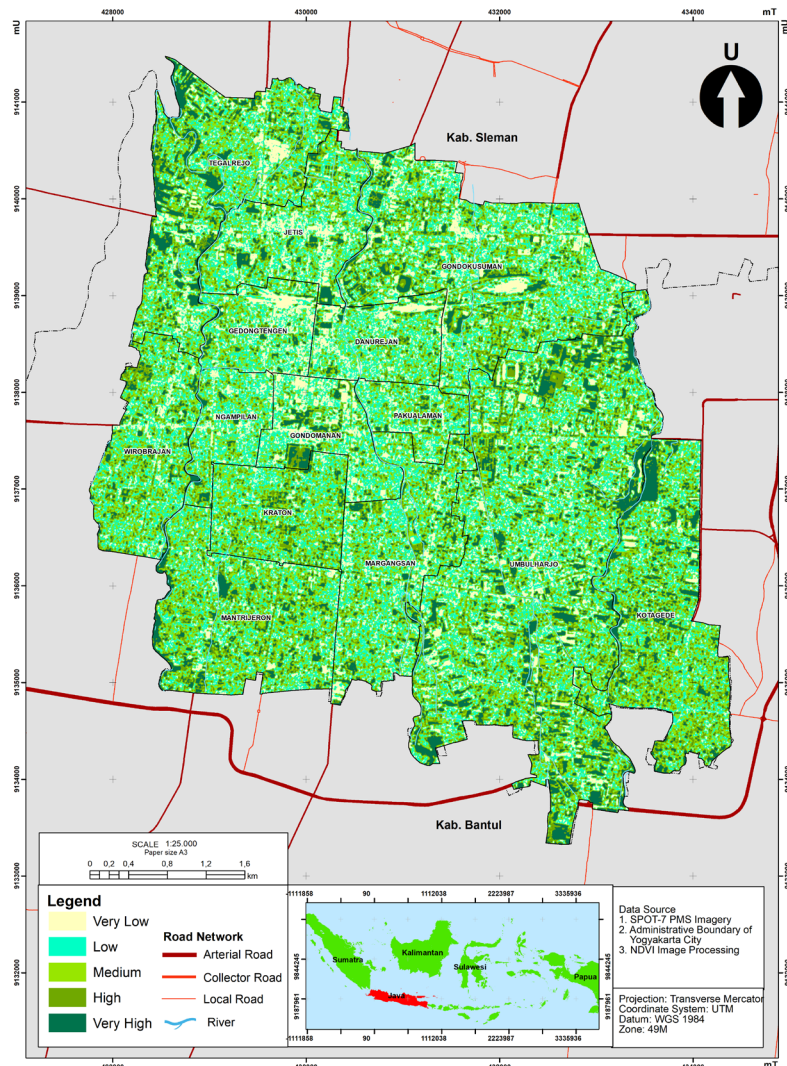
$$Cb = B \times \%C \text{ Organic} \dots \dots \dots (2.4)$$

where:

Cb : Carbon stock (kg)
 B : Biomass (kg)
 %C Organic : Percent carbon content (0.46)
 Source : Mardiana et al. (2018)

3. Results and Discussion

Image Transformation: Vegetation Index Values



Images cropped to fit the administrative boundaries of Yogyakarta City were inputted to ENVI and transformed using the selected vegetation index, the Normalized Difference Vegetation Index (NDVI). Figure 2 shows the results of the NDVI-based transformation. The NDVI values for the city varied from -0.5986 to 1.00, which, as the map shows, were distributed into five ranges or classes of vegetation abundance: very low (-0.5986–0.1725), low (0.1725–0.2916), medium (0.2916–0.4358), high (0.4358–0.6176), and very high (0.6176–1.0). Spatially, the very low abundance class covered an area of 522.63 ha, low 1,039.87 ha, medium 867.88 ha, high 538.41 ha, and very high 334.91 ha.

In Yudistira et al. (2019), NDVI values lower than 0.1041 correspond to water bodies, barren lands, settlements, and paved roads, while those between 0.1041 and 0.3667 represent vegetation and barren areas without asphalt, between 0.3667 and 0.5214 indicate plantations, golf courses, and reeds, and higher than 0.5214 are mainly forests. Observations of vegetation abundance on the NDVI image revealed that very low values (-0.5986–0.1725) were non-green open space objects, while low, medium, high, and very high values (0.1725–1.00) indicated green open space. These results are in line with the findings of Wiradharma et al. (2014), which classified $0.1 < \text{NDVI} < 1$ as vegetation and $-1 < \text{NDVI} < 0.1$ as non-vegetation objects. The derived levels of vegetation


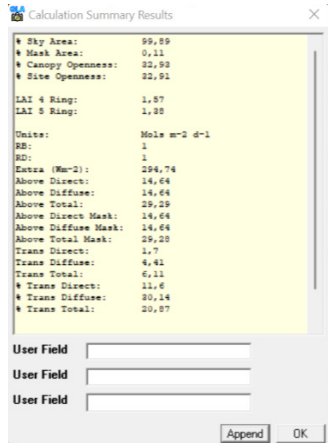
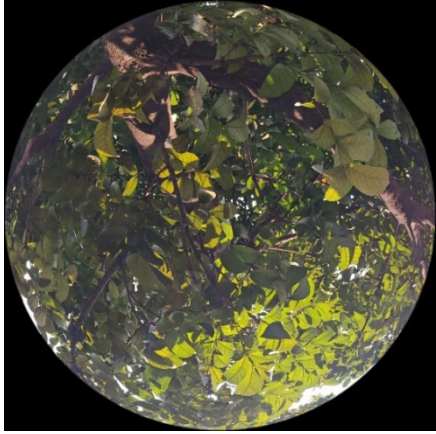
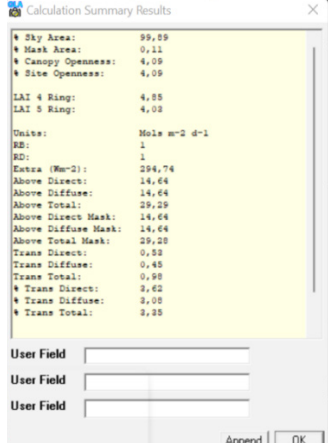
abundance were then compared to actual density in the field to statistically examine the relationship between NDVI and canopy density.

Actual Vegetation Density

Actual vegetation density was inferred from the existing percent tree canopy cover photographed and measured in each field sample plot. Field samples were determined using stratified random sampling. For the vegetation density validation test and the actual biomass calculation, the sample size was 42 stands that were randomly distributed in each class of vegetation abundance in Yogyakarta City. The test was conducted in a $3 \times 3 \text{ m}^2$ sample plot, and the canopy photos were taken using a fisheye lens because it has wider coverage than a regular camera.

To accommodate the field survey, the NDVI map was cropped to only display images of vegetation stands, which were classified as green open spaces. Based on the NDVI results, green open space is indicated by four classes: low, medium, high, and very high; very low values were excluded as they correspond to objects other than green open space. The information obtained in the field ensured that only vegetation with a canopy was used to validate the classified density or abundance.

Table 4. Samples of percent canopy density processing in the Gap Light Analyzer software

Sample	Image from Fish Eye lens	Processing result
2		
40		

Source: Data analysis, 2022

The canopy photos were inputted into the Gap Light Analyzer (GLA) software to calculate the %canopy cover (vegetation density). Several advantages of GLA are that the value of the canopy cover can be directly analyzed from field photos captured using a hemispherical (fisheye) lens and that it helps produce accurate calculations (Andriansah, 2020). Moreover, canopy cover can be classified more quickly when the photos have good quality, i.e., color contrast between the sky and the canopy; therefore, a threshold setting should be adjusted accordingly to increase the contrast for clear color boundaries (Frazer et al., 1999). In this study, the pixel value for the threshold was set at 130 for the entire samples. Percent tree canopy cover was obtained by subtracting %canopy openness from 100% (entirely covered by the canopy). %canopy openness is the percentage of unobscured skies visible in a canopy photo. Results showed the lowest vegetation density of 52.52% with an NDVI value of 0.3962 and the highest density of 95.91% with an NDVI value of 0.8987. Table 4 presents some photo samples of canopy density in the field and their processing results in GLA.

Actual Biomass

As proposed by Kish (1965), the number of samples used for research in a large population is at least between 30 and 200, and it should represent each identified class. Therefore, the biomass was calculated using 42 samples, which were also

used in the vegetation density validation test. Most of the samples were located in community-owned plantation areas with both natural and cultivated plants. However, some were in public areas, such as the Gajah Wong Educational Park, the Gembira Loka Zoo, and green median strips. Moreover, not all sample locations were easily accessible by vehicles or on foot, making it necessary to expand or shift the sample plots to obtain trunk measurements.

Based on field surveys, 109 tree trunks were identified in the entire sample plots to represent all classes of vegetation density. The measurements were performed on all species of woody stands, meaning that grasses, shrubs, and trees belonging to other species (e.g., banana plants) were not considered. The DBH values converted from the trunk circumference were analyzed using an allometric equation to estimate the tree's biomass and ability to absorb CO₂ emissions.

Table 4 shows that the biomass produced in each sample plot varied from 0.0196 to 3.5702 tonnes/pixel, amounting to 32.7659 tonnes/pixel. The highest biomass was found in sample no. 16, while the lowest was in sample no. 6. The amount of biomass is influenced by the number and diameter of stands in a given area. In addition, species also affect the biomass they produce because different species have different trunk diameters and leaf structures. Stands with a large diameter and high abundance produce a high amount of biomass, and vice versa. However, some locations where a few trees with a

fairly large tree diameter grow may have fairly high biomass, as found in sample no. 28, where the identified two stands with a DBH of 31.21 cm and 28.03 cm contained 1.5125 tonnes/pixel biomass. In addition, Table 5 shows that the carbon storage

of the samples also varied from 0.0098 to 1.7851 tonnes/pixel, with a total carbon storage of 15.0723 tonnes/pixel produced from 46% of the tree stand biomass.

Table 5. Biomass and carbon stock calculated from field-derived data

Sample	Coordinate		Number of trees	Actual Biomass (tonnes/pixel)	Actual Carbon Stock (tonnes/pixel)
	X	Y			
1	428379	9138237	2	0.2391	0.1100
2	429500	9135624	4	1.2976	0.5969
3	432022	9135641	2	0.0273	0.0126
4	432552	9139418	2	0.3067	0.1411
5	428633	9136418	1	0.4911	0.2259
6	428968	9140685	5	0.0196	0.0090
7	431341	9134713	3	1.5425	0.7095
8	430739	9136846	1	0.2300	0.1058
9	431625	9135519	3	1.1716	0.5389
10	433565	9135132	5	1.1515	0.5297

Table 5. Biomass and carbon stock calculated from field-derived data (continued)

Sample	Coordinate		Number of trees	Actual Biomass (tonnes/pixel)	Actual Carbon Stock (tonnes/pixel)
	X	Y			
11	430997	9138533	1	0.3099	0.1426
12	433166	9134286	2	0.0716	0.0330
13	433612	9137465	2	0.3327	0.1530
14	431244	9139026	2	1.1038	0.5077
15	432679	9134852	1	0.0412	0.0190
16	431573	9137752	2	3.5702	1.6423
17	432273	9135228	5	0.5550	0.2553
18	430052	9137294	1	0.7726	0.3554
19	432250	9135046	6	1.1738	0.5399
20	433437	9135249	2	1.3192	0.6068
21	432552	9138195	3	0.5791	0.2664
22	431261	9135627	2	0.2009	0.0924
23	431822	9134818	3	1.7296	0.7956
24	430676	9139980	3	2.0158	0.9273
25	428538	9140445	2	0.7676	0.3531
26	428890	9141127	2	0.8269	0.3804
27	429459	9139299	2	0.1735	0.0798
28	432603	9138378	2	1.5125	0.6957
29	433137	9135827	4	1.1564	0.5319
30	434047	9136735	3	0.0516	0.0237
31	432968	9133833	2	0.3909	0.1798
32	428684	9141168	4	1.2822	0.5898
33	429132	9140435	3	0.0668	0.0307
34	431571	9138623	3	0.7472	0.3437
35	429308	9139324	1	0.0697	0.0321
36	430794	9139266	2	1.4300	0.6578
37	433563	9137102	7	1.4436	0.6641
38	433062	9134121	1	0.5228	0.2405
39	432973	9138037	2	1.1131	0.5120
40	430175	9139019	2	0.4101	0.1887
41	428818	9138917	2	0.2686	0.1236
42	432973	9137857	2	0.2797	0.1287

Source: Data analysis, 2022

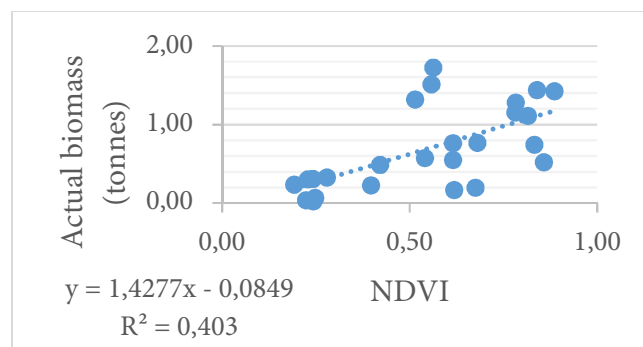


Figure 3. Scatter diagram of the linear regression model between NDVI and actual biomass

Statistical Analysis

The data were tested for normality using the Kolmogorov-Smirnov method, with a significance value of > 0.05 . Results showed that the significance values of canopy density and actual biomass data were 0.180 and 0.135; both are greater than 0.05, indicating normal distribution. Afterward, the data were examined statistically with correlation and regression analysis. The correlation analysis showed a positive correlation between the NDVI value and actual canopy density, with a Pearson correlation coefficient of 0.668 ($p = 0.000 < 0.05$), and between NDVI and actual biomass, with a Pearson correlation coefficient of 0.635 ($p = 0.001 < 0.05$). In other words, NDVI is related to both canopy density and biomass. Based on the degree of relationship proposed by Astuti (2017), these coefficients are within the range of 0.40–0.70, suggesting a medium correlation in a five-scale classification (very weak, weak, medium, strong, satisfactory).

The linear regression analysis results between NDVI and actual biomass are visually shown in the scatter diagram in Figure 3. Results showed a coefficient of determination or R-squared (R^2) of 0.403, which means that the NDVI value can only explain or model 40.3% of the variation in biomass, while other factors shape the remaining 59.7%. This figure can be influenced by the condition of the image used, especially as a result of image corrections and image cutting, which can affect the average pixel value and, thus, the vegetation index value. According to Margaretha *et al.* (2013), one of the problems in estimating urban carbon using remote sensing is that the built-up land generally covers a larger area than the vegetated land; consequently, the spectral value of the built-up land pixels tends to dominate that of vegetation. This affects the value of the resulting vegetation index.

Biomass Estimation Model's Accuracy Test

The resulting regression model was tested for accuracy using Root Mean Squared Error (RMSE), which demonstrates the model's degree of error. Low RMSE values mean minor errors in the estimation model. The accuracy test (17 validation samples) used a different sample size from the model (25 modeling samples). The regression model generated between NDVI and actual biomass had an RMSE value of 0.4853, suggesting a difference of 0.4853 tonnes/pixel between the observed and the modeled biomass. Because this figure is not significantly far from zero (0), the model is concluded as having good accuracy. This result was further confirmed by the RMSE-observations Standard Deviation Ratio (RSR) value of 0.5472. Based on the RSR category by Moriasi *et al.* (2007),

it is in the range of 0.50–0.60, indicating a model with good performance.

Biomass and Carbon Stock Estimates

Biomass in Yogyakarta City was calculated using the simple linear regression equation generated for NDVI value and biomass: $y = 1.4277x - 0.0849$. Here, 1.4277 is a coefficient value that shows an increase in NDVI will affect the biomass value by 1.4277 units, while -0.0849 , a constant, means the biomass decreases by 0.0849 regardless of changes in the NDVI value. This equation was used to estimate the biomass of a vegetation stand from the aboveground parts: trunks and leaves of woody trees. Based on the estimation results, Yogyakarta City had four classes of biomass density: low (0.1613–0.5644 tonnes/pixel), medium (0.5644–0.7776 tonnes/pixel), high (0.7776–0.9629 tonnes/pixel), and very high (0.9629–1.3428 tonnes/pixel), as shown in Figure 4.

The distribution of carbon stock estimates within the districts' administrative boundaries in Yogyakarta City is mapped in Figure 5 and presented in more detail in Table 5. The highest amounts of biomass and carbon stock were produced in Umbulharjo, while the lowest were in Pakualaman. Further, Table 6 shows a total biomass of 1,399,487.1 tonnes in the entire city. The estimated biomass was further used to calculate the carbon stock.

The total carbon stored in Yogyakarta City was estimated at 643,764.1 tonnes. This number is substantially different from the results of Margaretha *et al.* (2013), in which vegetation stands in the city and its surroundings stored 303,667.8 tonnes of carbon, as estimated using NDVI values derived from the ALOS AVNIR-2 image. Such a significant difference (340,096.3 tonnes) can be due to the different image characteristics used in both studies. Margaretha *et al.* used multiple-year images with a 10m resolution (medium resolution), while the current study used a higher spatial resolution (1.5 m); such differences affect the classified vegetation area and the sample plot size. In another study by Apriadna (2018), the aboveground biomass of tree stands in Magelang City and its surroundings was 3,019,944 tonnes, which is higher than the estimated biomass in this study. Magelang has an area of 1,812 ha, narrower than Yogyakarta, 3,250 ha. This proves that area does not affect the amount of biomass and carbon stock. In addition, this research also used SPOT-7, which is different from the Sentinel-2A image used in Apriadna's study. Table 7 shows the total carbon stock of each district in Yogyakarta City.

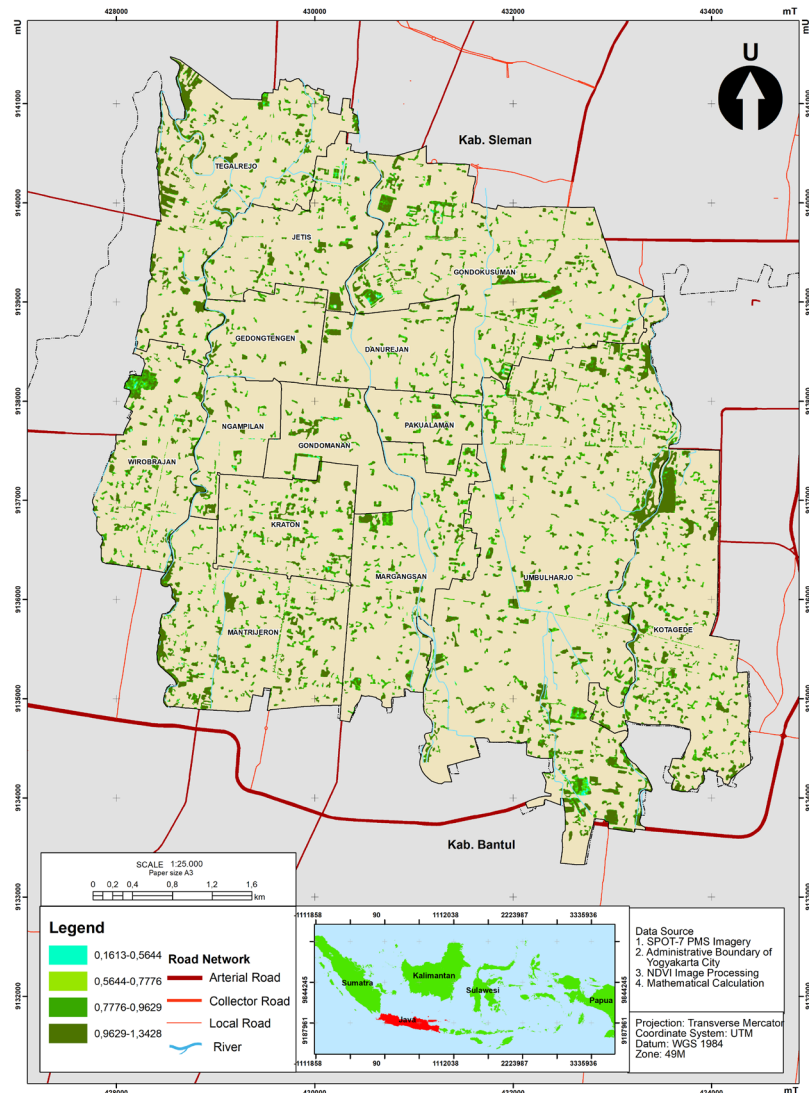


Figure 4. Map of biomass estimates for each class of vegetation density in Yogyakarta City

Table 6. Biomass per district in Yogyakarta City

Number	District	Biomass (tonnes)
1	Danurejan	27,784.55
2	Gedongtengen	24,342.85
3	Kraton	54,733.77
4	Mantriweron	130,141.50
5	Jetis	58,034.95
6	Kotagede	166,442.00
7	Pakualaman	18,545.89
8	Tegalrejo	165,327.90
9	Margangsari	80,393.31
10	Ngampilan	23,152.35
11	Umbulharjo	359,338.00
12	Wirobrajan	87,898.42
13	Gondokusuman	175,708.90
14	Gondomanan	27,642.72

Source: Data analysis, 2022

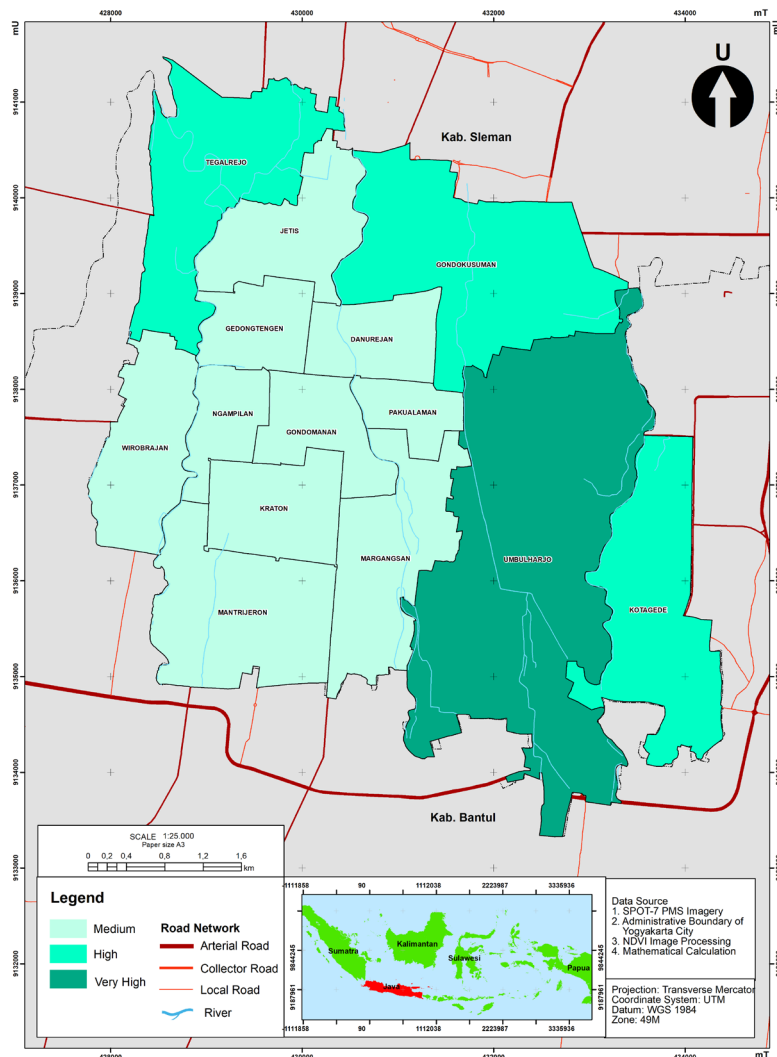


Figure 5. Map of carbon stock estimates for each district in Yogyakarta City

Table 7. Estimated biomass and carbon stock for each district in Yogyakarta City

District	Total Biomass (tonnes)	Total Carbon Stock (tonnes)
Danurejan	27,784.55	12,780.89
Gedongtengen	24,342.85	11,197.71
Kraton	54,733.77	25,177.53
Mantriweron	130,141.50	59,865.09
Jetis	58,034.95	26,696.07
Kotagede	166,442.00	76,563.32
Pakualaman	18,545.89	8,531.10
Tegalrejo	165,327.90	76,050.83
Margangsana	80,393.31	36,980.92
Ngampilan	23,152.35	10,650.08
Umbulharjo	359,338.00	16,5295.48

Table 7. Estimated biomass and carbon stock for each district in Yogyakarta City (continued)

District	Total Biomass (tonnes)	Total Carbon Stock (tonnes)
Wirobrajan	87,898.42	40,433.27
Gondokusuman	175,708.90	80,826.09
Gondomanan	27,642.72	12,715.65
Total	1,399,487.10	643,764.10

Source: Data analysis, 2022

Table 8. CO₂ absorption for each sub-district in Yogyakarta City

District	Total CO ₂ Absorption (tonnes)
Danurejan	46,863.27
Gedongtengen	41,058.27
Kraton	92,317.62
Mantrijeron	219,505.33
Jetis	97,885.62
Kotagede	280,732.17
Pakualaman	31,280.73
Tegalrejo	278,853.05
Margangsan	135,596.72
Ngampilan	39,050.29
Umbulharjo	606,083.43
Wirobrajan	148,255.34
Gondokusuman	296,362.34
Gondomanan	46,624.05
Total	2,360,468.30

Source: Data analysis, 2022

Aside from carbon stock, the estimated biomass was also used to determine its potential absorption of CO₂ emissions as a causing factor of air pollution. The equation used comprises the Relative Molecular (Mr) and Relative Atomic (Ar) values of CO₂. Table 8 presents the biomass and the absorption of CO₂ emissions in each city's district in detail. It shows that the vegetation stands in Yogyakarta could absorb 2,360,468.3 tonnes of CO₂ emissions. This indicates that vegetation has an essential role in capturing and storing carbon to reduce air pollution in urban areas.

The results of this study are in the form of estimates that do not entirely reflect the actual figures in the field; therefore, other variables are needed to improve the predicted values. In addition, the plant's absorption capacity was only calculated for vegetation stands, particularly woody trees, excluding other species of vegetation, such as shrubs and grasses, that also contain carbon. This study considered tree stands because they produce more significant biomass, store more carbon, and thus have a higher absorption capacity. Therefore, it is suggested that future research calculates carbon stock using other variables, diverse parameters, and different types of images to support and complement the results of this study.

4. Conclusion

Estimations using remote sensing and statistical analysis for Yogyakarta City showed NDVI values between -0.5986 and 1.00 and vegetation stands that produce 1,399,487.1 tonnes and store up to 643,764.1 tonnes of carbon. Based on districts, Umbulharjo has the highest carbon stock, while Pakualaman has the lowest. These results are, however, in the form of estimates that do not entirely reflect the actual figures on the ground. Therefore, other variables are needed to increase the accuracy and performance of the estimation model. In addition, this study calculated biomass for only one type of vegetation, i.e., stands or woody trees, excluding other species such as shrubs and grasses that also contain carbon because woody trees produce a more significant amount of biomass, store more carbon, and have a higher absorption capacity.

Therefore, estimating carbon stock using other parameters is recommended to complement this study's results.

Acknowledgment

The authors would like to thank the National Institute of Aeronautics and Space for providing satellite imagery data and the final recognition grant for the financial support, allowing the completion of this research. In addition, the preparation of this research cannot be separated from the role of many people and institutes who provided invaluable assistance, guidance, and support during field surveys and research activities. The authors would, therefore, like to express their gratitude to these parties.

References

- Achmad, E, Nursanti, Manalu, JHB (2018). Model Spasial Pendugaan Biomassa di Atas permukaan Tanah di Hutan Nagari Padang Limau Sundai Kabupaten Solok Selatan Provinsi Sumatera Barat, *Jurnal Silva Tropika*, vol. 2(3), pp. 67-76.
- Andriansah, R (2020). Analisis Kondisi Mangrove Berdasarkan NDVI (Normalized Difference Vegetation Index) dan Tutupan Kanopi Menggunakan Citra Sentinel-2 di Pulau Payung, Muara Sungai Musi, Banyuasin, Sumatera Selatan, *Skripsi*, Fakultas Matematika dan Ilmu Pengetahuan Alam, Universitas Brawijaya: Malang.
- Apriadna, R (2018). Estimasi Volume Oksigen Ruang Terbuka Hijau di Kota Magelang dan Sekitarnya, *Skripsi*, Fakultas Geografi, Universitas Gadjah Mada: Yogyakarta.
- Astuti, CC (2017). Analisis Korelasi untuk Mengetahui Keeratan Hubungan antara Keaktifan Mahasiswa dengan Hasil Belajar Akhir. *Journal of Information and Computer Technology Education*, vol. 1(1), pp. 1-7.
- Ayvaz, B, Kusakci, AO, & Temur, GT (2017). Energy-related CO₂ Emission Forecast for Turkey and Europe and Eurasia: a Discrete Grey Model Approach, *Grey Systems: Theory and Application*, vol. 7(3), pp. 436-452.
- BPS (2021a). *Provinsi Daerah Istimewa Yogyakarta dalam Angka 2021*, Jakarta: BPS.
- BPS (2021b). *Kota Yogyakarta dalam Angka 2021*, Jakarta: BPS.

- Brown, S (1997). *Estimating Biomass and Biomass Change of Tropical Forests: a Primer*, FAO Forestry Paper, vol. 5(4).
- Cooley, T, Anderson, GP, Felde, GW, Hoke, ML, Ratkowski, AJ, Chetwynd, JH, & Lewis, P (2002). FLAASH, a MODTRAN4-based Atmospheric Correction Algorithm, Its Application and Validation. *IEEE*, pp.1414-1418.
- Danoedoro, P (2012), *Pengantar Penginderaan Jauh Digital*, ANDI, Yogyakarta.
- Fibriawati, L 2016. Koreksi Atmosfer Citra SPOT-6 Menggunakan Metode MODTRAN4. *Seminar Nasional Penginderaan Jauh*, pp. 98-146.
- Frazer, GW, Canham, CD, & Lertzman, KP (1999). *Gap Light Analyzer (GLA), Version 2.0: Imaging software to extract canopy structure and gap light transmission indices from true-colour fisheye photographs, users manual and program documentation*, New York: Simon Fraser University.
- Handayani, CN, Sukmono, A, & Firdaus, HS (2020). Analisis Ketersediaan Ruang Terbuka Hijau Terhadap Emisi CO₂ Oleh Gas Buang Kendaraan Bermotor di Kelurahan Tembalang dan Sumurboto, *Jurnal Geodesi Undip*, vol. 9(2), pp. 198-207.
- Hung, T (2000). *MODIS Application in Monitoring Surface Parameters*, Institute of Industrial Science: Tokyo.
- Irawan, S & Sirait, J (2018). Perubahan Kerapatan Vegetasi Menggunakan Citra Landsat 8 di Kota Batam Berbasis Web, *Jurnal Kelautan*, vol. 10(2), pp. 174-184.
- Jensen (2014). *Remote Sensing of The Environment: An Earth Resource Perspective Second Edition*, Pearson Education Limited: USA.
- Jiaojun, Y, Yushi, C & Ye, Z (2008). *Effect on Atmospheric Correction by Inputting Parameters of Model*. Remote Sensing Application.
- Kish, L (1965). *Survey Sampling*, Michigan: John Wiley & Sons.
- Krisnawati, H, Adinugroho, WC, & Imanuddin, R (2012). *Monograf Model-Model Alometrik untuk Pendugaan Biomassa Pohon pada Berbagai Tipe Ekosistem Hutan di Indonesia*, Bogor: Badan Penelitian dan Pengembangan Konservasi dan Rehabilitasi-Kementerian Kehutanan dan Lingkungan Hidup.
- Lee, HY (2008). An Analysis on development capacity of an urbanized area for urban growth management, *Journal of the Korean Urban Geographical Society*, vol. 11(1), pp. 1-18.
- Lee, ZH, Sethupathi, S, Lee, KT, Bhatia, S, & Mohamed, AR (2013). An Overview on Global Warming in Southeast Asia: CO₂ Emission Status, Efforts Done, and Barriers, *Renewable and Sustainable Energy Reviews*, vol. 28, pp. 71-81.
- Leprieur, C, Kerr, YH, Mastorchio, S & Meunier, JC (2000). Monitoring vegetation cover across semi-arid regions: comparison of remote observations from various scales, *International Journal of Remote Sensing*, vol. 21(2), pp.281-300.
- Lu, D (2005). The Potential and Challenge of Remote Sensing-Based Biomass Estimation. *International Journal of Remote Sensing*, vol. 27(7), pp. 1297-1328.
- Ma, S, He, F, Tian, D, Zou, D, Yan, Z, Yang, Y, Zhou, T, Huang, K, Shen, H, & Fang, J (2018). Variations and Determinants of Carbon Content in Plants: A Global Synthesis, *Biogeosciences*, vol. 15(3), pp.693-702.
- Mansur, M & Pratama, BA (2014). Potensi Serapan Gas Karbondioksida (CO₂) pada Jenis- Jenis Pohon Pelindung Jalan (Potential Absorption of Carbon Dioxide (CO₂) in Wayside Trees), *Jurnal Biologi Indonesia*, vol. 10(2), pp. 149-158.
- Mardiana, G, Udiansyah, & Pitri, RMN (2018). Potensi Simpanan dan Serapan Karbon di Tas Permukaan Tanah pada Kawasan Hutan Desa Sungai Bakar Kecamatan Bajuin, *Jurnal Sylva Scientiae*, vol. 1(1), pp.56-64.
- Margaretha, EW, Danoedoro, P, & Murti, SH (2013). Estimasi Cadangan Karbon Vegetasi Tegakan di Kota Yogyakarta dan Sekitarnya Berbasis ALOS AVNIR-2, *Prosiding Simposium Nasional Sains Geoinformasi*, pp. 431-440.
- Moriassi, DN, Arnold, JG, Liew, MWV, Bingner, RL, Harmel, RD, & Veith, TL (2007). Model evaluation guidelines for systematic quantification of accuracy in watershed simulations, *Transactions of the ASABE*, vol. 50(3), pp.885-900.
- Mukono, J (2011). *Aspek Kesehatan Pencemaran Udara*, Surabaya: Airlangga University Press.
- Noor, A (2018). Perbandingan Algoritma Support Vector Machine Biasa dan Support Vector Machine Berbasis Particle Swarm Optimization untuk Prediksi Gempa Bumi, *Jurnal Humaniora dan Teknologi*, vol. 4(1), pp. 31-37.
- Nowak, DJ, Greenfield, EJ, Hoehn, RE & Lapoint, E (2013). Carbon storage and sequestration by trees in urban and community areas of the United States, *Environmental pollution*, vol.178, pp.229-236.
- Qanitat, F (2016). *Jogja One Park Rampung Akhir 2017*, diakses pada 6 Maret 2022, <https://ekonomi.bisnis.com/read/20160327/48/531666/jogja-one-park-rampung-akhir-2017>.
- Samsuodin, I, Dharmawan, IWS, & Siregar, A (2009). Potensi Biomassa Karbon Hutan Alam dan Hutan Bekas Tebangan Setelah 30 Tahun di Hutan Penelitian Malinau, Kalimantan Timur, *Jurnal Penelitian Hutan dan Konservasi Alam*, Vol. IV(1), pp. 47-56.
- Siregar, S (2015). *Statistika Parametrik Untuk Penelitian Kuantitatif Dilengkapi Dengan Perhitungan Manual dan Aplikasi SPSS Versi 17*, Jakarta: Bumi Aksara.
- Solima, S (2010). *Electrical Load Predictioning*, Elsevier Inc, United States.
- SPOT 6/7 daya user's community 2013, *SPOT 6/7 Imagery - User Guide*, France: Airbus Defence and Space Intelligence.
- Sutaryo, D (2009). *Perhitungan Biomassa, Sebuah Pengantar untuk Studi Karbon dan Perdagangan Karbon*, Wetlands International Indonesia Programme: Bogor.
- Sutanto (1986). *Penginderaan Jauh Jilid 1*, Yogyakarta: Gadjah Mada University Press.
- The European Space Agency n.d., *SPOT 7*, Earth Online, <https://earth.esa.int/eogateway/missions/spot-7>.
- Usman, H dan Akbar, PS (2003), *Pengantar Statistika*, Jakarta: PT. Bumi Aksara.
- Wahrudin, U, Atikah, S, Al Habibah, A, Paramita, QP, Tampubolon, H, Sugandi, D, & Ridwana, R (2019). Pemanfaatan Citra Landsat 8 untuk Identifikasi Sebaran Kerapatan Vegetasi di Pangandaran, *Jurnal Kajian Ilmu dan Pendidikan Geografi*, vol. 3(2), pp. 90-101.
- Wahyuni, NI (2012). Integrasi Penginderaan Jauh dalam Perhitungan Biomassa Hutan, *Info BPK Manado*, vol. 2(2), pp. 115-126.
- Wijayanti, T (2015). Evaluasi Potensi Biomassa Hutan Berdasarkan Nilai Indeks Vegetasi Menggunakan Data Penginderaan Jauh (Studi Kasus: KPH Bojonegoro, Jawa Timur), *Tugas Akhir, Fakultas Teknik Sipil dan Perencanaan, Institut Teknologi Sepuluh Nopember*.
- Wiradharma, D, Sobirin, & Saraswati, R (2014), *Perubahan Kemampuan Serapan Karbon Dioksida (CO₂) Oleh Ruang Hijau di Kota Bogor*, Depok: Universitas Indonesia.
- Yanti, D, Megantara, I, Akbar, M, Meiwanda, S, Syauqi, IM, Sugandi, D, & Ridwana, R 2020, Analisis Kerapatan Vegetasi di Kecamatan Pangandaran Melalui Citra Landsat 8, *Jurnal Geografi, Edukasi dan Lingkungan (JGEL)*, vol. 4(1), pp. 32-38.
- Yudistira, R, Mecha, AI, & Prasetyo, SYJ (2019). Perubahan Konversi Lahan Menggunakan NDVI, EVI, SAVI dan PCA pada Citra Landsat 8 (Studi Kasus: Kota Salatiga), *Indonesian Journal of Computing and Modeling*, vol. 1, pp. 25-30.
- Yunkai & Zeng, F (2012). *Atmospheric Correction Modul QUAC and FLAASH User's Guide Version 4.7*. ITT Visual Information Solution Inc.
- Zhao, P, Zhou, Y, Li, F, Ling, X, Deng, N, Peng, S & Man, J (2020). The Adaptability of APSIM-Wheat Model in The Middle and Lower Reaches of Yangtze River Plain of China: A Case Study of Winter Wheat in Hubei Province, *Agronomy*, vol. 10, pp. 1-15.